Electronic structure calculations for a carbon nanotube capacitor with a dielectric medium

Kazuyuki Uchida and Atsushi Oshiyama
Department of Applied Physics, University of Tokyo, Hongo, Tokyo 113-8656, Japan
and CREST, Japan Science and Technology Agency, Sanbancho, Tokyo 102-0075, Japan
(Received 26 September 2008; revised manuscript received 11 May 2009; published 30 June 2009)

We report first-principles electronic structure calculations based on the density-functional theory (DFT) that reveal characteristic features of nanometer-scale capacitors consisting of triple-walled (TW) carbon nanotubes (CNTs). Calculated electron densities under bias voltages provide atom-scale clarifications of the dielectric responses of the intercalated CNT as well as quantum spill of the stored charge densities from the electrode CNTs. Our DFT-based analysis shows that redistribution of the electron density in the TWCNT under the bias voltage is essentially a superposition of the stored-charge distribution near the electrode CNTs and the dielectric-polarization-charge distribution due to the intercalated CNT. The dielectric polarization due to the intercalated CNT screens the electric field due to the stored charges and hereby enhances the electrostatic capacitance of the TWCNT capacitor. From the calculated capacitance, we estimate an effective dielectric constant of the intercalated CNT to be $\epsilon_{\infty}^{\mathrm{eff}} \sim 1.88$, a comparable value to SiO_2 which is widely used in the modern semiconductor devices. It is also clarified that the amount of the stored charge in the nanometer-scale capacitor is *not* obtained by spatial integration of the corresponding electron density owing to substantial overlap of the quantum spill and the polarization charge but should be defined through the amount of charges injected into particular electron states of each electrode. We also discuss a modification of the band gap of the TWCNT under the bias voltage in terms of the local variation in the electrostatic potential.

DOI: 10.1103/PhysRevB.79.235444 PACS number(s): 77.90.+k, 73.90.+f, 73.22.Dj

I. INTRODUCTION

Capacitance is a fundamental element in electronic devices. It plays an important part in the modern technology of field-effect transistors (FETs) in which a current flow along the channel region is controlled by a bias voltage applied to a capacitor between the channel and a gate electrode. Fabricable sizes of such capacitors approach to a nanometer scale in recent years, leading to an observation[1] of quantum-mechanical behavior in the capacitance of carbon nanotubes (CNTs) in a FET structure.

In nanometer-scale capacitors (nanocapacitors), charges are accommodated in particular electron states, and the spatial distribution of the charges is in a scale of nanometer, being comparable with the extent of each wave function. This renders quantum effects prominent in nanocapacitors. The electron states, on the other hand, are strongly affected by detailed atomic arrangements in nanometer-scale structures. Hence, in order to analyze, understand, and predict characteristics of nanometer-scale capacitors, knowledge as to the atomic and electronic structures is imperative. It is thus obvious that reliable and atomistic calculations play important roles in clarifying the quantum behavior of nanocapacitors.

In fact, several calculations which clarify the quantum behavior on the basis of the density-functional theory (DFT) are available. Tanaka *et al.*[2] have calculated the capacitance between two jellium electrodes with nanometer-scale vacuum gap and found an enhancement of the capacitance compared with what is expected from the classical electromagnetism. This enhancement is attributable to electron (quantum) spill from the electrodes. We have obtained the enhancement also in a double-walled CNT capacitor[3] and clarified that the amount of the quantum spill is determined by the response of each electron state of the CNT electrodes under the electric field. We have also found that one-dimensional Van-Hove singularities peculiar to the density of states (DOS) of the CNT structure cause drastic variation in the capacitance as a function of the bias voltage. This bias-voltage dependence of the capacitance in nanocapacitor has been observed indeed.[1]

Those calculations have predicted and clarified some aspects of quantum behavior in nanocapacitors. Yet they have been performed for the electrodes separated by vacuum. In usual situations, dielectrics are intercalated between the electrodes. It is thus of importance to reveal the dielectric response of the intercalated dielectric under the electric field due to the stored charges. Further, the interface between the electrode and the dielectric is also expected to be crucial in determining the properties of nanocapacitors. When the intercalated dielectric is of nanometer scale, reliable first-principles calculations may be the most powerful tool to reveal its dielectric response.

Multiwalled carbon nanotubes (MWCNTs) which are nanometer-scale coaxial-cylindrical-structured materials are commonly recognized as promising materials for channels of transistors in future electronics. This is due to their mechanical robustness and the capability of carrying larger currents under required electric fields than conventional Si or Ge. In future electronics, the surrounding-gate transistors (SGT) (Refs. 4 and 5) in which the channel and the gate form nanometer-scale coaxial cylinders may be an ultimate structure of FETs. Hence, MWCNT may be a material which realizes this ultimate FET. When they are used as SGTs, the inner and outer CNTs are contacted by leads and work as electrodes of the capacitor whereas the intercalated CNTs with adequate band gaps work as dielectrics. Further, structural peculiarity of MWCNTs offer a representative stage to consider quantum effects in nanocapacitors including the re-

sponses of the dielectric and the characteristics of the electrode-dielectric interface.

In the present work, we consider a triple-walled CNT (TWCNT) as a representative of MWCNTs and clarify its quantum behavior as a nanoscale capacitor based on the density-functional theory.[6] We take (8,0) and (27,0) semiconductor CNTs as electrodes in which charges are stored due to the applied bias voltages. The (17,0) CNT is intercalated between the two electrode CNTs and play a role of dielectric. Issues that we consider are (i) how the electrons in the dielectric (intercalated CNT) respond to the electric field due to the bias voltage and the stored charge in the electrodes (inner and outer CNTs), and (ii) how we define the amount of the stored charge in nanocapacitors. We actually calculate a redistribution of the electrons in the capacitor under a bias voltage, and show that the redistribution of the electrons is essentially explained by a superposition of the stored charge in the CNT electrodes and the dielectric-polarization charge in the intercalated CNT with their considerable overlapping at the interface regions. We point out that the amount of the stored charge should be calculated from the changes in the band filling of each CNT electrode and is *never* estimated from a spatial integration of the electron redistribution due to this overlapping. The electric field between the CNT electrodes is partially screened by the dielectric polarization of the intercalated CNT leading to an enhancement of the electrostatic capacitance. We estimate an effective dielectric constant of the intercalated CNT to be $\epsilon_{\infty}^{\mathrm{eff}} \sim 1.88$, which describes this screening. We also point out that the band-gap width of the TWCNT is changed by the bias application due to the electrostatic shifts of the band structures among the CNTs.

The organization of the paper is as follows: we introduce our model and method in Sec. II. The results and discussions are shown in Sec. III. We finally summarize our findings in Sec. IV.

II. MODEL AND METHOD

Figure 1 shows the atomic structure of the TWCNT (8,0)@(17,0)@(26,0) nanocapacitor that we study in the present work. We consider that the (8,0) and (26,0) zigzag CNTs are electrodes of the nanocapacitor so that finite bias voltage μ is applied between them. The (17,0) zigzag CNT is a dielectric intercalated between these CNT electrodes. The difference in the roles of these three CNTs is assured by the band structure of the TWCNT, which will be discussed in the following of the paper. The radius of the (8,0), (17,0), and (26,0) CNTs are 3.16, 6.64, and 10.1 Å, respectively. The interwall spacing of the coaxial CNTs is ~3.4 Å, known to be an optimum CNT-CNT distance from previous investigations.[7] It is thus recognized that the present system is a plausible model of nanoscale CNT capacitors with the interelectrode spacing filled with a dielectric CNT. An experimental technique to obtain such a multiwalled capacitor structure contacted by leads has been proposed.[8]

In practical calculations, we use a supercell model in which an infinite-length TWCNT capacitor is placed in a cell with enough vacuum region, and each cell is arranged in a hexagonal lattice with the lattice constants of $a=32$ Å and $c=4.3$ Å. The lattice constant c corresponds to the common periodicity of the (8,0), (17,0), and (26,0) CNTs along the tube directions. In the directions perpendicular to the tube axes, each TWCNT is separated by at least 11 Å from adjacent TWCNTs. This separation of the capacitors ensures that electron distribution is confined within each capacitor. Also, electric field exists only between the two electrodes in each capacitor. Interactions among the capacitor and its mirrors in the supercell model are thus safely negligible and our supercell model describes a single TWCNT capacitor isolated in vacuum. The unit cell contains 204 carbon atoms, which are sum of the 32 atoms in the (8,0) CNT, the 68 atoms in the (17,0) CNT, and the 104 atoms in the (26,0) CNT.

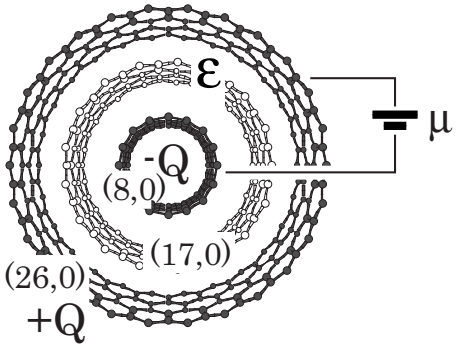

FIG. 1. Atomic structure of the TWCNT, (8,0)@(17,0)@(26,0), as a nanoscale coaxial-cylindrical capacitor with a dielectric medium. The (8,0) and (26,0) CNTs are electrodes of the TWCNT capacitor, and the (17,0) CNT is a dielectric intercalated between them. The difference in the roles played by these three CNTs is assured by the band structures (Figs. 2 and 6) of the TWCNT with and without the bias voltage μ.

Calculations are performed within the local-density approximation (LDA) (Ref. 9) in the DFT (Ref. 6). The interpolation formula for the exchange-correlation energy[10] fitted for the Monte Carlo results[11] is utilized. Nuclei and core electrons are simulated by the ultrasoft pseudopotentials.[12] Kohn-Sham orbitals are expressed by a plane-wave basis set with the cutoff energy of 25 Ry. All calculations are done at 0 K and the DOS is calculated using the tetrahedron method without using the smearing technique. Atomic positions are optimized under the zero-bias voltage, $\mu=0$. Computations are performed with the aid of the program package, TAPP.[13]

Our calculation of the capacitor under a finite bias voltage is performed with a constraint on the band filling of each CNT. To explain our scheme, we first describe the band structure of the (8,0)@(17,0)@(26,0) TWCNT. Figure 2 shows (a) the band structure of the TWCNT without applying the bias voltage ($\mu=0$), along with (c) the energy bands of each constituent CNT. We find that the TWCNT is a narrow-gap semiconductor under the zero-bias voltage with the energy gap of $E_g=0.082$ eV, which is indicated by the shaded region in Fig. 2, whereas the constituent (8,0), (17,0), and (26,0) CNTs have the energy gaps of 0.60, 0.57, and 0.36 eV, respectively. The energy bands of the constituent CNTs [Fig. 2(c)] along with the TWCNT [Fig. 2(a)] are aligned with the common vacuum level. We find that the energy bands of the thinner CNT shift downward compared to those

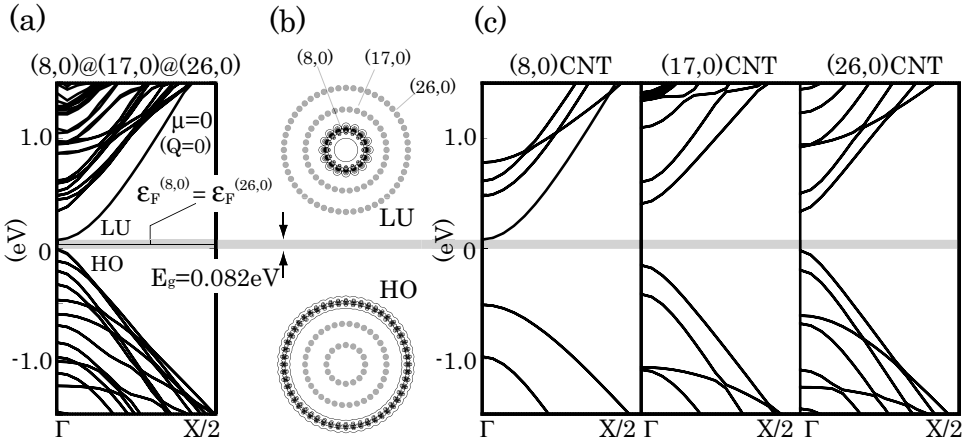

FIG. 2. (a) Band structure of the (8,0)@(17,0)@(26,0) TWCNT capacitor without applying the bias voltage (μ=0). The system is a narrow-gap semiconductor with the band gap of E_g=0.082 eV. The Fermi levels of the (8,0) and (26,0) CNT electrodes, $\epsilon_F^{(8,0)}$ and $\epsilon_F^{(26,0)}$, are both supposed to be located at the midgap position of the TWCNT when μ=0. The amount of the stored charge is Q=0. (b) Distributions of the squared wave functions of the lowest LU state and the highest HO state. (c) Band structure of isolated (8,0), (17,0), and (26,0) CNTs. The vacuum levels of the CNTs are the same in these figures.

of thicker CNT. The band structure of the TWCNT is essentially explained by a superposition of the band structures of these three CNTs, except for slight modifications induced by the inter-CNT interactions.[14] By comparing Figs. 2(a) and 2(c), we find that the bottom of the conduction band of the TWCNT is originated from the inner (8,0) CNT whereas the top of the valence band is from the outer (26,0) CNT. This is evidenced by Fig. 2(b) which shows that the wave functions of the lowest-unoccupied (LU) and the highest-occupied (HO) states of the TWCNT are distributed mainly on the inner (8,0) and the outer (26,0) CNTs, respectively. No electron state in the vicinity of the band gap of the TWCNT is originated from the intercalated (17,0) CNT. These band alignments of the CNTs are explained by a combination of the band-gap narrowing in the larger-radius CNT (Ref. 15) and the downward shift of the conduction band due to the σ^*-π^* hybridization in the smaller-radius CNTs.[16]

To discuss the capacitance, it is necessary to obtain the electronic structures of the capacitor with a finite bias voltage between the two electrodes, (8,0) and (26,0) CNTs. Alternatively, it is required to fill one electrode with some electrons with a negative charge ($-Q$) and the other electrode with some holes with a positive charge ($+Q$), and then obtain the electronic structure of the capacitor in this situation. The characteristic feature of the energy bands of the (8,0)@(17,0)@(26,0) TWCNT as described above facilitates these calculations using a constraint-LDA technique (see Appendix): we inject extra electrons $-Q$ into the bottom of the conduction bands (LU states) and extra holes $+Q$ into the top of the valence bands (HO states), and perform iterations for obtaining the self-consistent field with this constraint on the band filling; this filling corresponds to filling of the minus charge $-Q$ in the (8,0) CNT electrode and the plus charge $+Q$ in the (26,0) CNT electrode since the LU and the HO states distribute on the inner (8,0) and the outer (26,0) CNTs, respectively. There is no charge injection into the intercalated dielectric of the (17,0) CNT,[17] and total-charge neutrality of the system is maintained in the present scheme ($+Q-Q$=0). The bias voltage μ is calculated as $\mu=\epsilon_F^{(8,0)}-\epsilon_F^{(26,0)}$, where $\epsilon_F^{(8,0)}$ and $\epsilon_F^{(26,0)}$ are the Fermi levels of the inner (8,0) and the outer (26,0) electrodes, respectively. In our scheme, the bias voltage μ is an output quantity as a function of the input stored charge Q. In the following descriptions, however, we use the bias voltage μ to specify the condition of the calculations for the sake of readability. When $\mu > E_g$, the Fermi level of the (8,0) [(26,0)] CNT electrode, $\epsilon_F^{(8,0)}$[$\epsilon_F^{(26,0)}$], is located in the conduction (valence) band of the (8,0) [(26,0)] CNT.[18]

The LDA is known to underestimate the energy gap, which may cause corrections of the quantitative values of the bias voltage μ in the Q-μ relation.

III. RESULTS AND DISCUSSION

Figure 3 shows the bias-induced redistribution of the electron density $\Delta\rho^{8@17@26}(\boldsymbol{r})$ in the TWCNT capacitor, (8,0)@(17,0)@(26,0), projected onto the cross section perpendicular to the CNT axes. The bias voltage applied between the (8,0) and (26,0) CNTs is μ=0.184 eV. Correspondingly, the amount of the stored charge is Q =0.03e/cell, where e denotes the elementary electric charge. The bias-induced redistribution is defined as

$$\Delta\rho^{8@17@26}(\boldsymbol{r}) = \rho_\mu(\boldsymbol{r}) - \rho_0(\boldsymbol{r}), \tag{1}$$

where $\rho_\mu(\boldsymbol{r})$ and $\rho_0(\boldsymbol{r})$ are the total electron densities in the TWCNT capacitor with and without, respectively, the bias voltage being applied. We find that the distribution of the induced charge $\Delta\rho^{8@17@26}(\boldsymbol{r})$ has a π-like character and the same periodicity as that in the atomic arrangement. We thus understand that the electron redistribution $\Delta\rho^{8@17@26}(\boldsymbol{r})$ reflects the atomic and electronic structures of the TWCNT. Figure 4(a) shows the radial distribution of $\Delta\rho^{8@17@26}(\boldsymbol{r})$, which is labeled as $\overline{\Delta\rho}^{8@17@26}(r)$, where $r(=|\boldsymbol{r}|)$ is the radial coordinate measured from the central axis of the TWCNT structure. The vertical dashed lines indicate the radii of the (8,0), (17,0), and (26,0) CNTs, respectively. We also draw a

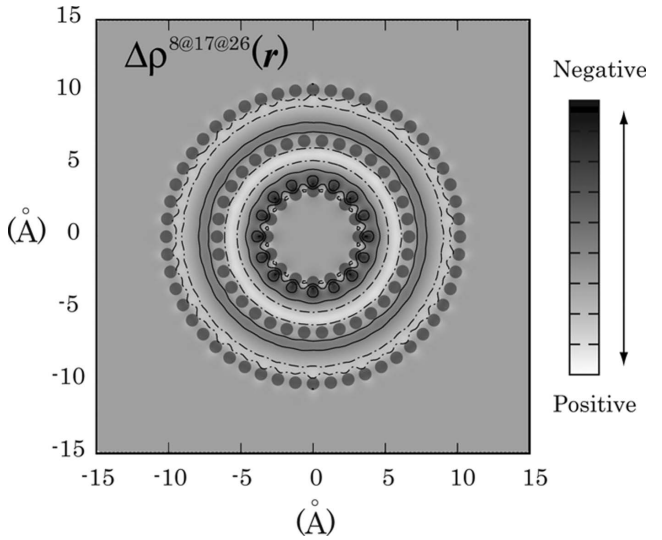

FIG. 3. Bias-induced redistribution of the electron density in the TWCNT capacitor, $\Delta\rho^{8@17@26}(\boldsymbol{r})$, projected onto the cross section perpendicular to the CNT axes. Gray circles denote carbon atoms. Solid- and dot-dashed lines are contour lines of the electron redistribution in the negatively and positively charged regions, respectively. The bias voltage μ between the (8,0) and (26,0) CNTs is $\mu=0.184$ eV. The amount of the stored charge is $Q=0.03e/\text{cell}$.

vertical thin solid line at $r=r_0$, where the radial redistribution $\overline{\Delta\rho}^{8@17@26}(r)$ is vanishing.

We find that the inner surface of the outer electrode [(26,0) CNT] is positively charged and the outer surface of the inner electrode [(8,0) CNT] is negatively charged. Also, the inner and outer surfaces of the intercalated dielectric [(17,0) CNT] are charged positively and negatively, respectively. As is shown below, these features correspond to a simple picture of polarization of capacitors in the classical electromagnetism, where the dielectric-polarization charges ($\mp\delta$) are induced at the interfaces between the electrodes and the dielectric due to the external charges ($\pm Q$) stored in the electrodes. First, let us consider a (8,0)@(26,0) double-walled carbon nanotube (DWCNT) capacitor, which is obtained by removing the dielectric (17,0) CNT from the TWCNT capacitor. Figure 4(b) shows the calculated electron redistribution $\overline{\Delta\rho}^{8@26}(r)$ in thus obtained DWCNT capacitor, (8,0)@(26,0), in which the same amount of charge Q ($=0.03e/\text{cell}$) as the TWCNT capacitor is stored. We find that the stored charge in the inner (outer) CNT electrode is spilt outward (inward) from the tube wall radius.[3] We then calculate the difference in the electron redistributions between the TWCNT capacitor and the DWCNT capacitor,

$$\overline{\Delta\rho}^{\text{sub}}(r)=\overline{\Delta\rho}^{8@17@26}(r)-\overline{\Delta\rho}^{8@26}(r), \tag{2}$$

as is shown in Fig. 4(c). Next, we consider an isolated (17,0) CNT which is under a radial electric field induced by two model electrodes: one is a positively charged cylindrical shell ($+Q=0.03e/\text{cell}$) with the radius of the (26,0) CNT and the other is a negatively charged cylindrical shell ($-Q=-0.03e/\text{cell}$) with the radius of the (8,0) CNT; both the shells have the width of 0.2 Å. This obviously mimics the intercalated (17,0) CNT between the outer (26,0) and the inner (8,0)

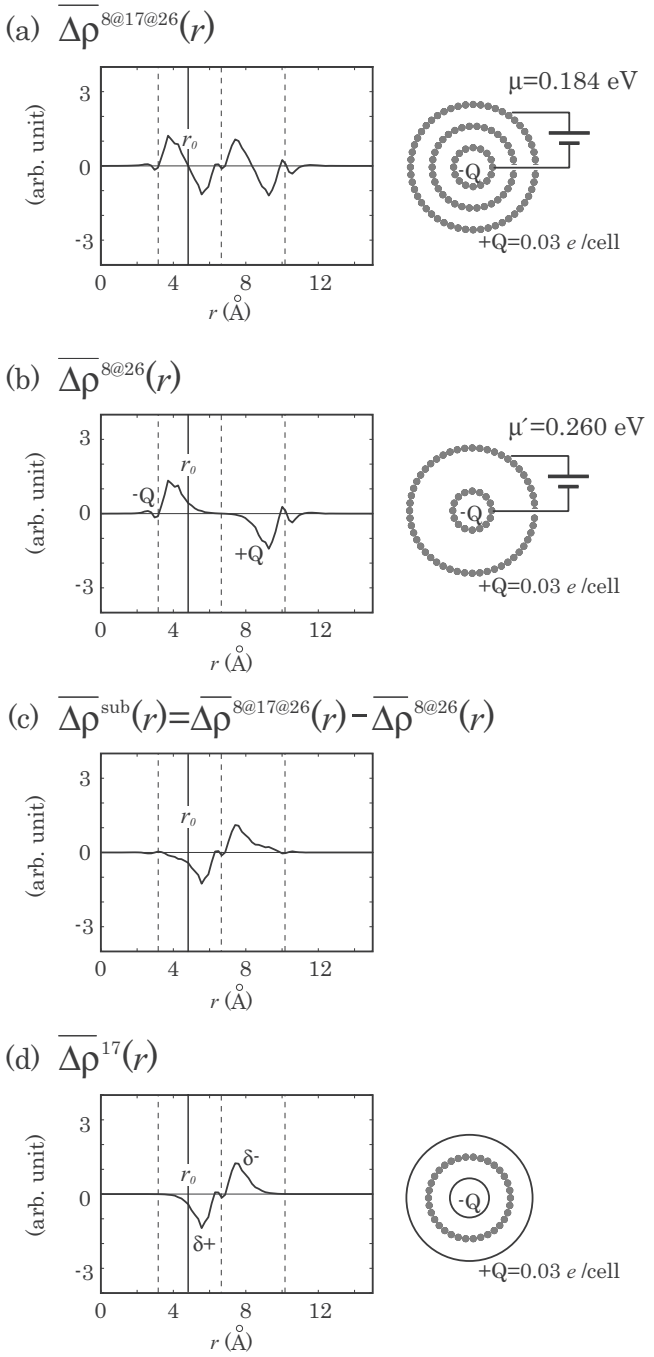

FIG. 4. A radial distribution of the induced electron density in (a) the (8,0)@(17,0)@(26,0) TWCNT capacitor, $\overline{\Delta\rho}^{8@17@26}(r)$ and that in (b) the (8,0)@(26,0) DWCNT capacitor, $\overline{\Delta\rho}^{8@26}(r)$. In both (a) and (b), the amount of the stored charge is $Q=0.03e/\text{cell}$. The bias voltage between the (8,0) and (26,0) CNTs is $\mu=0.184$ eV in (a) and $\mu'=0.260$ eV in (b), respectively. (c) Difference between (a) and (b), $\overline{\Delta\rho}^{\text{sub}}(r)=\overline{\Delta\rho}^{8@17@26}(r)-\overline{\Delta\rho}^{8@26}(r)$. (d) Dielectric-polarization charge $\overline{\Delta\rho}^{17}(r)$ of a (17,0) CNT under a radial electric field between a positively charged cylindrical shell ($+Q=+0.03e/\text{cell}$) with the (26,0) CNT's radius and a negatively charged cylindrical shell ($-Q=-0.03e/\text{cell}$) with the (8,0) CNT's radius. Both the shells have the width of 0.2 Å. In [(a)–(d)], three vertical dashed lines indicate the radii of the (8,0), (17,0), and (26,0) CNTs, respectively. A vertical thin solid line at $r=r_0$ shows a zero-point radius of $\overline{\Delta\rho}^{8@17@26}(r)$.

CNTs which are charged with the amount of $\pm 0.03e$/cell. We calculate the electron density of the (17,0) CNT under this field as well as the density without the field and then obtain the density difference between them, i.e., polarization-charge density, $\overline{\Delta\rho}^{17}(r)$, of the (17,0) CNT under the electric field, which is shown in Fig. 4(d).

It is clear from Figs. 4(c) and 4(d) that $\overline{\Delta\rho}^{\mathrm{sub}}(r)$ and $\overline{\Delta\rho}^{17}(r)$ are very similar to each other. We thus understand that the electron redistribution $\Delta\rho^{8@17@26}(\boldsymbol{r})$ in the TWCNT capacitor is essentially explained by a superposition of the stored charge $\Delta\rho^{8@26}(\boldsymbol{r})$ in the (8,0) and (26,0) CNTs, and the dielectric-polarization charge $\Delta\rho^{17}(\boldsymbol{r})$ in the intercalated (17,0) CNT,

$$\Delta\rho^{8@17@26}(\boldsymbol{r}) = \Delta\rho^{8@26}(\boldsymbol{r}) + \Delta\rho^{\mathrm{sub}}(\boldsymbol{r}) \sim \Delta\rho^{8@26}(\boldsymbol{r}) + \Delta\rho^{17}(\boldsymbol{r}). \tag{3}$$

The slight difference between the distributions of $\overline{\Delta\rho}^{\mathrm{sub}}(r)$ and $\overline{\Delta\rho}^{17}(r)$ is ascribed to the bias-induced variations in the orbital hybridization between the adjacent CNTs.[19] We find that this difference is not prominent, compared with the stored charge $\Delta\rho^{8@26}(\boldsymbol{r})$ in the (8,0) and (26,0) CNTs nor the dielectric-polarization charge $\Delta\rho^{17}(\boldsymbol{r})$ in the intercalated (17,0) CNT.

In Fig. 4(a), we show the zero point of $\overline{\Delta\rho}^{8@17@26}(r)$ at the radius of $r=r_0$. The integrated value of $\overline{\Delta\rho}^{8@17@26}(r)$ within the cylinder defined by $r<r_0$ is calculated to be $\sim 0.02e$/cell, less than 70% of the injected charge Q $(=0.03e$/cell) into the electrode. This underestimate is obviously due to the considerable spatial overlapping of the stored charge $\overline{\Delta\rho}^{8@26}(r)$ in the (8,0)/(26,0) CNT [Fig. 4(b)] and the dielectric-polarization charge $\overline{\Delta\rho}^{17}(r)$ in the (17,0) CNT [Fig. 4(d)], around the radius of $r=r_0$. In previous calculations of nanoscale capacitors,[2,3,20] the amount of the stored charge Q has been defined by a spatial integration of the electron redistribution over some region. Yet the charge defined in such a way is *not* equal to the charge injected into the electrode owing to the charge overlapping at the electrode-dielectric interfaces, as is clearly demonstrated here. This unequality is discovered only when the interelectrode spacing is filled with a dielectric. Since the bias voltage or the corresponding charge injected into each electrode is the controllable quantity in experiments, our definition of the stored charge, i.e., the injected charge into the electron states of each electrode, is certainly relevant. The appropriate definition of the stored charge Q is essential in discussing the capacitance precisely.

The electron redistribution in the TWCNT with the application of the bias voltage causes a variation in the electrostatic potential. We calculate the variation in the potential by

$$\Delta V^{8@17@26}(\boldsymbol{r}) = V_{\mu}(\boldsymbol{r}) - V_0(\boldsymbol{r}), \tag{4}$$

where $V_{\mu}(\boldsymbol{r})$ and $V_0(\boldsymbol{r})$ are the electrostatic potentials with and without the bias voltage μ, respectively. Figure 5(a) shows an averaged value of $\Delta V^{8@17@26}(\boldsymbol{r})$ at the radial coordinate of $r(=|\boldsymbol{r}|)$, which is labeled as $\overline{\Delta V}^{8@17@26}(r)$ hereafter. The bias voltage between the (8,0) and (26,0) CNT electrodes is $\mu=0.184$ eV. The vertical dashed lines indicate the radii of the (8,0), (17,0), and (26,0) CNTs, respectively. We

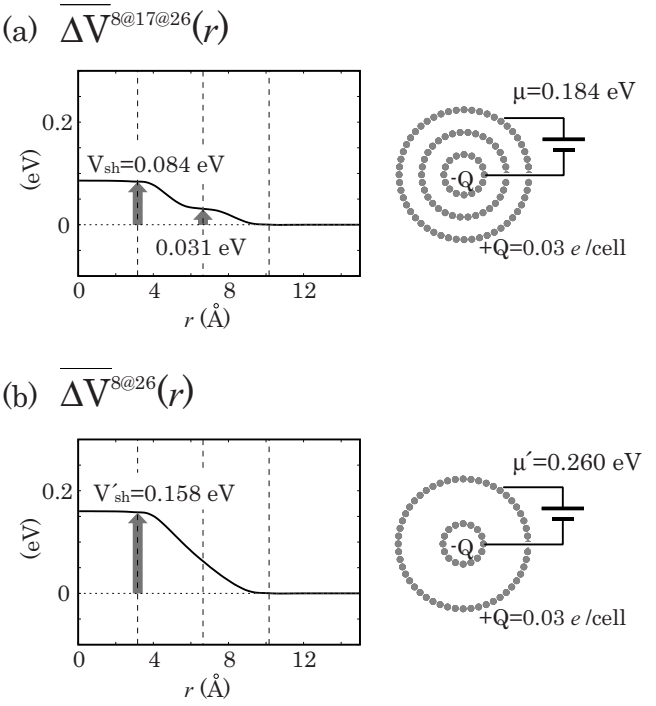

FIG. 5. An averaged value of the electrostatic potential in (a) the MWCNT capacitor and (b) the DWCNT capacitor, plotted as a function of the radial coordinate $r(=|\boldsymbol{r}|)$ measured from the CNT axes. The potential shift between the (8,0) and (26,0) CNTs is $V_{\mathrm{sh}}=0.084$ eV in (a) and $V'_{\mathrm{sh}}=0.158$ eV in (b), respectively. The amount of the stored charge is $Q=0.03e$/cell in both (a) and (b). The bias voltage is $\mu=0.184$ eV in (a) and $\mu'=0.260$ eV in (b), respectively. Three vertical dashed lines indicate the (8,0), (17,0), and (26,0) CNT radii, respectively.

find that the potential level at the (8,0) CNT is shifted upward by 0.084 eV with respect to the (26,0) CNT. We label this shift as V_{sh} hereafter. The potential level at the (17,0) CNT dielectric is also shifted upward by 0.031 eV. It is noteworthy that the calculated potential shift of $V_{\mathrm{sh}}=0.084$ eV is definitely smaller than the applied bias voltage of $\mu=0.184$ eV. This is because a part of the applied bias voltage μ is used to overcome the finite band gap $E_g(=0.082$ eV) of the TWCNT [Fig. 2(a)] and because the shift of the Fermi level of each electrode (within the DOS spectrum) upon the charge accommodation is finite in nanoscale capacitors.[3] This difference between the applied bias voltage μ and the potential shift V_{sh} leads to a result that contributions from the DOS of the electrodes are also included in the total capacitance $(C=dQ/d\mu)$ of nanoscale systems, in addition to the electrostatic capacitance $(C_0=dQ/dV_{\mathrm{sh}})$. Such a contribution of the DOS of the electrode has been discussed theoretically[3,21] and is actually observed experimentally.[1] We do not discuss this point any more in the present work, however, as the present paper is focused on the responses of the dielectric to the electric field and the properties of the dielectric-electrode interfaces.

The gradient of the potential $\overline{\Delta V}^{8@17@26}(r)$ corresponds to the electric field. As shown in Fig. 5(a), we find that the slope of the potential $\overline{\Delta V}^{8@17@26}(r)$ is relatively steep at the interface regions between the inner and the intercalated

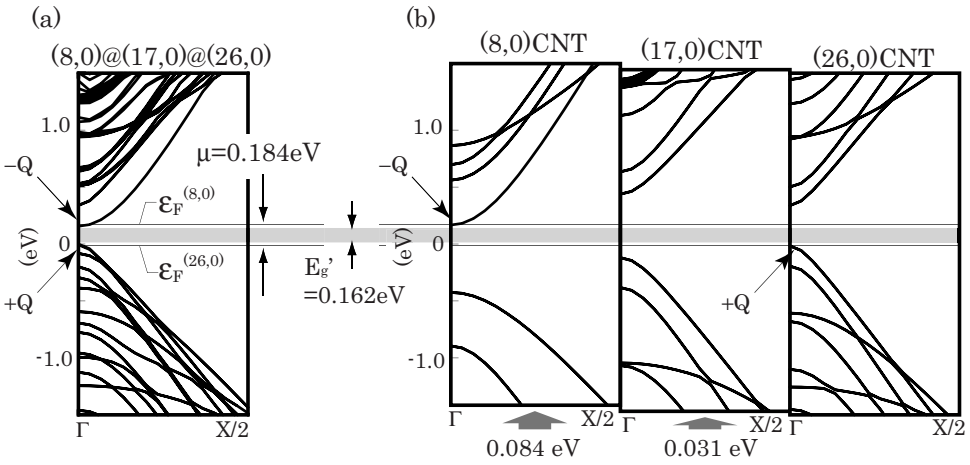

FIG. 6. (a) Band structure of the TWCNT capacitor under the bias voltage of $\mu(=\epsilon_F^{(8,0)}-\epsilon_F^{(26,0)})=0.184$ eV, which is essentially explained by a superposition of (b) the band structure of an isolated (26,0) CNT, and those of the (8,0) and (17,0) CNTs with the upward shifts of 0.084 and 0.031 eV, respectively. Two horizontal thin lines show the Fermi level of the (8,0) CNT electrode, $\epsilon_F^{(8,0)}$, and that of the (26,0) CNT electrode, $\epsilon_F^{(26,0)}$, respectively. The shaded region indicates the band gap $[E_g'=0.162$ eV$(<\mu)]$ of the TWCNT under this bias voltage. The bottom of the conduction band of the (8,0) CNT electrode is injected with electrons $(-Q=-0.03e/\text{cell})$ and the top of the valence band of the (26,0) CNT electrode is occupied by holes $(+Q=+0.03e/\text{cell})$. The (17,0) CNT is a dielectric intercalated between these CNT electrodes with no charge injected because both $\epsilon_F^{(8,0)}$ and $\epsilon_F^{(26,0)}$ are located in the energy gap of the (17,0) CNT.

CNTs, and between the outer and the intercalated CNTs while the potential is rather flat around the intercalated (17,0) CNT. Such behavior of the potential $\Delta V^{8@17@26}(r)$ is due to the screening of the electric field by the dielectric polarization of the (17,0) CNT intercalated between the (8,0) and (26,0) CNT electrodes. To elucidate the role of the dielectrics, we calculate the electrostatic potential $\Delta V^{8@26}(r)$ in the (8,0)@(26,0) DWCNT capacitor in which the same amount of charge Q $(=0.03e/\text{cell})$ as in the TWCNT capacitor is stored [Fig. 5(b)]. As shown in Fig. 5(b), the gradient of the potential in the DWCNT capacitor is larger than that in the TWCNT capacitor [Fig. 5(a)]. This is clearly because there is no screening by the (17,0) CNT in the DWCNT capacitor. The potential shift V_{sh}' at the inner (8,0) tube with respect to the outer (26,0) tube is calculated to be $V_{\text{sh}}'=0.158$ eV in the DWCNT capacitor.

The screening of the electric field is reflected on the electrostatic capacitance C_0 which is defined as

$$C_0 = \frac{dQ}{dV_{\text{sh}}}. \tag{5}$$

As the amount of the stored charge Q is proportional to the the bias voltage V_{sh} at least within the calculated bias range, the electrostatic capacitance is also calculated by

$$C_0 \sim \frac{Q}{V_{\text{sh}}}. \tag{6}$$

In the (8,0)@(17,0)@(26,0) TWCNT capacitor, the calculated value of the potential shift is $V_{\text{sh}}=0.084$ eV when the amount of the stored charge is $Q=0.03e/\text{cell}$. Hence, the electrostatic capacitance of the TWCNT is $C_0=0.134\times10^{-19}$ F/Å. In the (8,0)@(26,0) DWCNT capacitor, on the other hand, the potential shift for the same amount of stored charge Q $(=0.03e/\text{cell})$ is calculated to be $V_{\text{sh}}'=0.158$ eV. Using these values, the electrostatic capacitance of the DWCNT is $C_0'=0.0714\times10^{-19}$ F/Å. It is clear that the electrostatic capacitance of the TWCNT capacitor is enhanced by the (17,0) CNT dielectric intercalated between the (8,0) and (26,0) CNT electrodes. Taking a ratio of the electrostatic capacitances obtained for the TWCNT and DWCNT capacitors, an effective dielectric constant of the intercalated (17,0) CNT is calculated to be $\epsilon_\infty^{\text{eff}}=C_0/C_0'\sim1.88$. This value is comparable to the dielectric constant of SiO_2 (~4 in the static region and ~2 in the optical region) which is widely used in the modern semiconductor devices. We note that the effective dielectric constant ($\epsilon_\infty^{\text{eff}}\sim1.88$) of the intercalated (17,0) CNT is smaller than the measured dielectric constant of bulk graphite[22] along the c axis in the optical region ($\epsilon_\infty^{\text{gra}}=4.5$). We speculate that this difference is attributed to the interlayer electron redistribution in bulk graphite with the semimetallic character under an electric field, which obviously leads to the dielectric constant larger than the single-walled CNT dielectric.

Finally, we explain a variation in the band structures of the TWCNT induced by the bias application. Figure 6(a) shows the band structure of the TWCNT capacitor calculated under the bias voltage of $\mu=0.184$ eV. The bottom of the conduction band (LU) is occupied by 0.03 electrons per cell and the top of the valence band (HO) accommodates 0.03 holes per cell. The LU and HO states distribute on the (8,0) and (26,0) CNTs, respectively, similar to the case of $\mu=0$ [Fig. 2(b)]. Here, we find that the band gap of the system after the bias application is increased to be $E_g'=0.162$ eV [Fig. 6(a)] from the intrinsic value of $E_g=0.082$ eV without the bias application [Fig. 2(a)]. The increase in the band gap, $E_g'-E_g=0.08$ eV, agrees with the potential shift V_{sh} $(=0.084$ eV) [Fig. 5(a)] between the (8,0) and (26,0) CNTs.[23] This infers that the variation in the band gap is ascribed to the relative shift of the band structures between the (8,0) and (26,0) CNTs according to the local variation in the electro-

static potential. It is naturally expected that the energy band of the (17,0) CNT is also shifted according to the potential shift at the (17,0) CNT. To elucidate the role of the potential shift, we present the band structures of the isolated (8,0) and (17,0) CNTs shifted upward by 0.084 and 0.031 eV, respectively, with respect to the band structure of the isolated (26,0) CNT [Fig. 6(b)].[24] The amount of the energy shifts are deduced from the potential shift at each radius of the corresponding CNT, as obtained from Fig. 5(a). We find that the band structure of the TWCNT after the bias application [Fig. 6(a)] is essentially identical to a superposition of these three band structures with the appropriate electrostatic energy shifts [Fig. 6(b)]. It is thus clarified that the modification of the band gap after the bias application is essentially due to the local shift of the electrostatic potential upon the bias application.

From Figs. 6(a) and 6(b), we also find that the Fermi levels of the (8,0) and (26,0) CNTs, $\epsilon_F^{(8,0)}$ and $\epsilon_F^{(26,0)}$, are certainly located in the conduction band of the (8,0) CNT and in the valence band of the (26,0) CNT, respectively. Both the Fermi levels are located in the band gap of the (17,0) CNT. This assures that the (8,0) and (26,0) CNTs are the electrodes of the TWCNT capacitor with the injected charges whereas the intercalated (17,0) CNT works as the dielectric of the capacitor, screening the electric field between the (8,0) and (26,0) CNT electrodes as is shown in Fig. 5(a).

IV. CONCLUSION

In conclusion, we have investigated the electronic structure of the (8,0)@(17,0)@(26,0) TWCNT as a nanoscale coaxial-cylindrical capacitor with a dielectric medium. We have shown that the redistribution of the electrons in the capacitor under the bias voltage is essentially explained by a superposition of the stored charge in the (8,0)/(26,0) CNT electrode and the dielectric-polarization charge in the (17,0) CNT. The electric field between the (8,0) and (26,0) CNT electrodes is partially screened by the dielectric polarization of the (17,0) CNT. The electrostatic capacitance of the TWCNT capacitor is enhanced due to this screening. The effective dielectric constant of the (17,0) CNT is estimated to be $\epsilon_\infty^{\mathrm{eff}}=C_0/C_0'\sim 1.88$, from the ratio of the electrostatic capacitance calculated for the (8,0)@(17,0)@(26,0) TWCNT capacitor and the (8,0)@(26,0) DWCNT capacitor. The band-gap width of the TWCNT is increased after the bias application due to the electrostatic shifts of the band structures among the CNTs. We have also pointed out that the amount of the stored charge Q should be calculated from the changes in the band filling of each CNT electrode and is *never* obtained from a spatial integration of the electron redistribution induced by the bias application. This is due to the considerable overlapping of the stored charge in the (8,0)/(26,0) CNT electrodes and the dielectric-polarization charge in the (17,0) CNT at the interface regions between these CNTs.

ACKNOWLEDGMENTS

This work was partly supported by grants-in-aid for scientific research from the Ministry of Education, Culture, Sports, Science, and Technology of Japan under Contracts No 17064002, No. 19054002, and No. 20740216. Computations were performed at Yukawa Institute of Theoretical Physics, Kyoto University, Cyber Media Center, Osaka University, Information Synergy Center, Tohoku University, Institute of Solid State Physics, Tokyo University, and Research Center of Computational Science, National Institute of Natural Sciences.

APPENDIX: CONSTRAINT-LDA APPROACH

In our constraint-LDA calculations, the electron density is expressed as a sum of the squared Kohn-Sham eigenfunctions $\psi_\epsilon(\mathbf{r})$ with the Kohn-Sham energy ϵ,

$$\rho(\mathbf{r}) = 2\sum_{\epsilon\le\epsilon_F^{\mathrm{v}}} |\psi_\epsilon(\mathbf{r})|^2 + 2\sum_{\epsilon^{\mathrm{cbb}}\le\epsilon\le\epsilon_F^{\mathrm{c}}} |\psi_\epsilon(\mathbf{r})|^2, \qquad \text{(A1)}$$

where ϵ^{cbb} is the energy at the conduction-band bottom.[25] The first term corresponds to the valence-band contribution and the second term to the conduction-band contribution. Quasi-Fermi levels, ϵ_F^{v} and ϵ_F^{c}, in the valence and conduction bands, respectively, are introduced to generate holes in the valence band in the energy range of $\epsilon_F^{\mathrm{v}}<\epsilon\le\epsilon_{\mathrm{vbt}}$ (the valence-band top), and electrons in the conduction band in the energy range of $\epsilon^{\mathrm{cbb}}\le\epsilon\le\epsilon_F^{\mathrm{c}}$. In each iteration to obtain the self-consistent field, the quasi-Fermi levels are determined so that the charge due to the accommodated holes (electrons) in the valence (conduction) band is $\pm Q$. The factor of 2 in Eq. (A1) corresponds to the spin degeneracy. Since the valence and the conduction bands of the (8,0)@(17,0)@(26,0) TWCNTs have characters of the outer (26,0) and the inner (8,0) CNTs, respectively, this constraint-LDA procedure precisely corresponds to the LDA calculation with a constraint that the holes and electrons with the magnitude of the charge Q are injected into the outer and the inner CNTs, respectively. In this sense, we write ϵ_F^{v} as $\epsilon_F^{(26,0)}$ and ϵ_F^{c} as $\epsilon_F^{(8,0)}$ in the text.

[1] S. Ilani, L. A. K. Donev, M. Kindermann, and P. L. McEuen, Nat. Phys. **2**, 687 (2006).

[2] M. Tanaka, Y. Gohda, S. Furuya, and S. Watanabe, Jpn. J. Appl. Phys., Part 2 **42**, L766 (2003).

[3] K. Uchida, S. Okada, K. Shiraishi, and A. Oshiyama, Phys. Rev. B **76**, 155436 (2007); see also K. Uchida, H. Kageshima, and H. Inokawa, *ibid.* **74**, 035408 (2006); K. Uchida and S. Okada, *ibid.* **79**, 085402 (2009).

[4] M. Masuoka, T. Endoh, and H. Sakuraba, *Proceedings of the Fourth IEEE International Caracas Conference on Devices, Cir-*

cuits, and Systems (IEEE, New York, 2002), pp. C015–1C015–5.

[5] H. Takato, K. Sunouchi, N. Okabe, A. Nitayama, K. Hieda, F. Horiguchi, and F. Masuoka, Tech. Dig.-Int. Electron Devices Meet. **1988**, 222; K. Sunouchi, H. Takato, N. Okabe, T. Yamada, T. Ozaki, S. Inoue, K. Hashimoto, K. Hieda, A. Nitayama, F. Horiguchi, and F. Masuoka, *ibid.* **1989**, 23.

[6] P. Hohenberg and W. Kohn, Phys. Rev. **136**, B864 (1964).

[7] S. Okada and A. Oshiyama, Phys. Rev. Lett. **91**, 216801 (2003).

[8] P. G. Collins, M. S. Arnold, and Ph. Avouris, Science **292**, 706 (2001).

[9] W. Kohn and L. J. Sham, Phys. Rev. **140**, A1133 (1965).

[10] J. P. Perdew and A. Zunger, Phys. Rev. B **23**, 5048 (1981).

[11] D. M. Ceperley and B. J. Alder, Phys. Rev. Lett. **45**, 566 (1980).

[12] D. Vanderbilt, Phys. Rev. B **41**, 7892 (1990).

[13] Tokyo *Ab initio* Program Package (TAPP) is developed by a consortium initiated at University of Tokyo: J. Yamauchi, M. Tsukada, S. Watanabe, and O. Sugino, Phys. Rev. B **54**, 5586 (1996); H. Kageshima and K. Shiraishi, *ibid.* **56**, 14985 (1997); O. Sugino and A. Oshiyama, Phys. Rev. Lett. **68**, 1858 (1992).

[14] W. Song, M. Ni, J. Lu, Z. Gao, S. Nagase, D. Yu, H. Ye, and Z. Zhang, Chem. Phys. Lett. **414**, 429 (2005).

[15] A graphene sheet, which can be regarded as a CNT with an infinite radius, has a zero band gap.

[16] X. Blase, L. X. Benedict, E. L. Shirley, and S. G. Louie, Phys. Rev. Lett. **72**, 1878 (1994).

[17] To guarantee that there is no charge injection into the intercalated (17,0) CNT, the quantity of the stored charge Q must be at most $\sim 0.1e/\text{cell}$. All calculations in this paper are performed for the charge Q less than this value.

[18] When the finite input charge $\pm Q$ is accommodated in the electrode CNTs, we definitely obtain the Fermi levels $\epsilon_F^{(8,0)}$ and $\epsilon_F^{(26,0)}$ as the outputs. We then calculate the bias voltage as $\mu = \epsilon_F^{(8,0)} - \epsilon_F^{(26,0)}$. When $Q=0$ and μ is in the range of $0 \leq \mu \leq E_g$, with $\epsilon_F^{(8,0)}$ and $\epsilon_F^{(26,0)}$ located somewhere in the band gap of the TWCNT. In this case, exact positions of $\epsilon_F^{(8,0)}$ and $\epsilon_F^{(26,0)}$ are not well defined. We thus define that $\epsilon_F^{(8,0)} = \epsilon_F^{(26,0)}$ is located at the center of the energy gap when $\mu=0$ and $\epsilon_F^{(8,0)}$ $[\epsilon_F^{(26,0)}]$ moves to the bottom (top) of the conduction (valence) band when μ increases to E_g. The results presented in this paper are unaffected by the way of defining the Fermi levels in the case of $Q=0$. We restrict ourselves to the case of $\mu \geq 0$ in this paper.

[19] The orbital hybridization between the adjacent CNTs without the bias voltage is discussed in: V. Zolyomi, J. Koltai, A. Rusznyak, J. Kurti, A. Gali, F. Simon, H. Kuzmany, A. Szabados, and P. R. Surjan, Phys. Rev. B **77**, 245403 (2008). We note that the bias-induced variation in the orbital hybridization is a part of the dielectric responses.

[20] P. Pomorski, L. Pastewka, C. Roland, H. Guo, and J. Wang, Phys. Rev. B **69**, 115418 (2004).

[21] M. Büttiker, J. Phys.: Condens. Matter **5**, 9361 (1993).

[22] E. A. Taft and H. R. Philipp, Phys. Rev. **138**, A197 (1965).

[23] The slight difference between the potential shift V_{sh} (=0.084 eV) and the increase in the band gap $E_g' - E_g$ (=0.08 eV) is ascribed to small modifications of the band structures in each CNT.

[24] In Fig. 6, the energy bands of (a) the TWCNT and (b) the constituent CNTs are first aligned with the common vacuum level. Then, the energy bands of the (8,0) and (17,0) CNTs are shifted upward by 0.084 and 0.031 eV, respectively.

[25] As we use the ultrasoft pseudopotential method in the present paper, Eq. (A1) is slightly modified according to the treatments shown in Ref. 12 to compensate for the deficit charge.